

Improved Near-Surface Velocity Models from the Nechako Basin Seismic Survey, South-Central British Columbia (Parts of NTS 93B, C, F, G), Part 2: Full-Waveform Inversion

B.R. Smithyman, Department of Earth and Ocean Sciences, University of British Columbia, Vancouver, BC, bsmithyman@eos.ubc.ca

R.M. Clowes, Department of Earth and Ocean Sciences, University of British Columbia, Vancouver, BC

Smithyman, B.R. and Clowes, R.M. (2011): Improved near-surface velocity models from the Nechako Basin seismic survey, south-central British Columbia (parts of NTS 93B, C, F, G), part 2: full-waveform inversion; *in* Geoscience BC Summary of Activities 2010, Geoscience BC, Report 2011-1, p. 255–264.

Introduction

The goal of this project was to process first-arrival data from a multichannel vibroseis reflection survey in the Nechako Basin of south-central British Columbia (BC) to provide an improved near-surface velocity model. In Smithyman and Clowes (2010), we reported on travelttime-inversion results using two well-known travelttime-inversion codes. We developed velocity models that, while potentially useful for interpretation in their own right, were designed primarily as inputs to a full-waveform inversion process. In this paper, we present subsurface velocity models generated by full-waveform inversion of these seismic data. Because they incorporate waveform amplitude and phase information, these velocity models are more detailed than the results of conventional near-surface refraction statics or ray-tracing. Additionally, the seismic first-arrival waveforms encode information about low-velocity zones in the near-surface region. Such zones are not modelled by travelttime codes, but are modelled in full-waveform inversion.

Vibroseis multichannel seismic acquisition is designed and tuned to produce high-quality near-offset reflection data. The application of refraction statics is normally used to account for near-surface heterogeneities when processing later arrivals, but the process can produce useful velocity models. In contrast, our travelttime-inversion efforts were designed primarily to produce high-quality velocity models using the extended offset data available from the 2008 Geoscience BC Nechako Basin vibroseis seismic survey (Calvert et al., 2009). The use of data from offsets of up to 14.4 km in the travelttime-inversion process provided velocity models with depths of investigation on the order of

2–3 km (dependent on local geology). Full-waveform inversion improves on the resolution and fidelity of the travelttime-inversion result by fitting the waveform amplitude and phase, instead of a single travelttime pick per trace.

Results from our studies (and the methodology that produced them) have relevance in the seismic processing and interpretation workflows for two main reasons: 1) interpretation can provide valuable information about the near-surface region that is not well parameterized by reflection methods; and 2) additional near-surface velocity information may be used to improve stacking and migration results through reprocessing procedures. Information from (1) can be helpful in identifying differing rock types and their relevance for further exploration, while that from (2) can enable improved images of the subsurface for better interpretation of geological structures, including those that may be associated with petroleum deposits.

Technical Background

We applied a technique known as waveform tomography, in which high-quality travelttime data are processed by travelttime (tomographic) inversion followed by frequency-domain, two-dimensional (2-D) acoustic full-waveform inversion of preconditioned waveform data (Pratt and Worthington, 1990; Pratt and Gouly, 1991; Pratt, 1999). This technique takes advantage of the reduced nonlinearity of the travelttime-inversion objective function compared to the objective function found in full-waveform inversion. By careful use of travelttime-inversion techniques, the full-waveform inversion process can begin close to the global minimum of the eventual solution.

The application of full-waveform inversion requires that the characteristics of the survey be reproduced accurately when generating synthetic data (forward modelling). This is simplest in cases where geometry and survey characteristics are regular or easily controlled; examples include synthetic studies, marine acquisition and cross-hole experi-

Keywords: *Nechako Basin, seismic surveys, seismic tomography, seismic inversion, first-arrival interpretation, waveform tomography, velocity models*

This publication is also available, free of charge, as colour digital files in Adobe Acrobat® PDF format from the Geoscience BC website: <http://www.geosciencebc.com/s/DataReleases.asp>.

ments. In these cases, the geometry of the survey can often be well parameterized and is frequently known to a high precision. Land acquisition in general, and vibroseis acquisition in particular, are more difficult to simulate in a 2-D full-waveform modelling code. This is because topographic features and land-use concerns often control the placement of shot points and receiver groups. The vibroseis method uses trucks with computer-controlled hydraulic vibrators to simulate the seismic response from an explosive source, but with less disruption and lower cost than explosives. This allows for denser and faster acquisition; hence, vibroseis is typically the preferred method for land-based exploration-seismic acquisition. The incorporation of off-line (y-direction) station offsets is often unavoidable. In the case of the Geoscience BC Nechako Basin seismic survey, the vibroseis trucks worked on the pre-existing logging roads in the area. The source and receiver geometries were controlled by the location of the roads, which in turn were determined by topography. The irregular geometries produce effects in the data that cannot be modelled correctly with a 2-D implementation.

The source characteristics of the vibroseis acquisition also provide advantages and disadvantages for full-waveform inversion. Vibroseis commonly allows for high signal-to-noise ratios through high-fold surveys and stacking of shots. The spatial sampling of the source locations is also potentially much finer, due to the speed and repeatability of vibroseis shooting. This is beneficial, especially with horizontally travelling waves, since the station spacing controls the maximum measurable frequency at wide azimuth. However, vibroseis seismic data are often band limited compared to data collected using an explosive source. The low-frequency signals that are very beneficial in full-waveform inversion are not typically included in the vibroseis sweep. The nominally zero-phase source signature must also be accounted for in processing and may affect the efficacy of waveform inversion at varying offsets. Finally, it is necessary to account for parameterization error in the survey geometry when applying the 2-D acoustic formulation of the wave equation.

We have developed a methodology for approaching 2-D waveform tomography of vibroseis data acquired along crooked roads. This incorporates approximations that are not necessary or desirable in a three-dimensional (3-D) full-waveform inversion workflow. Our goal was not to improve upon existing 3-D workflows, but rather to overcome obstacles that limited the effectiveness of 2-D waveform tomography in cases where the survey is not ideal.

Geological Background

The Nechako Basin is a sedimentary basin in the Intermontane Belt of the western Canadian Cordillera (Figure 1). This area has been characterized as prospective for

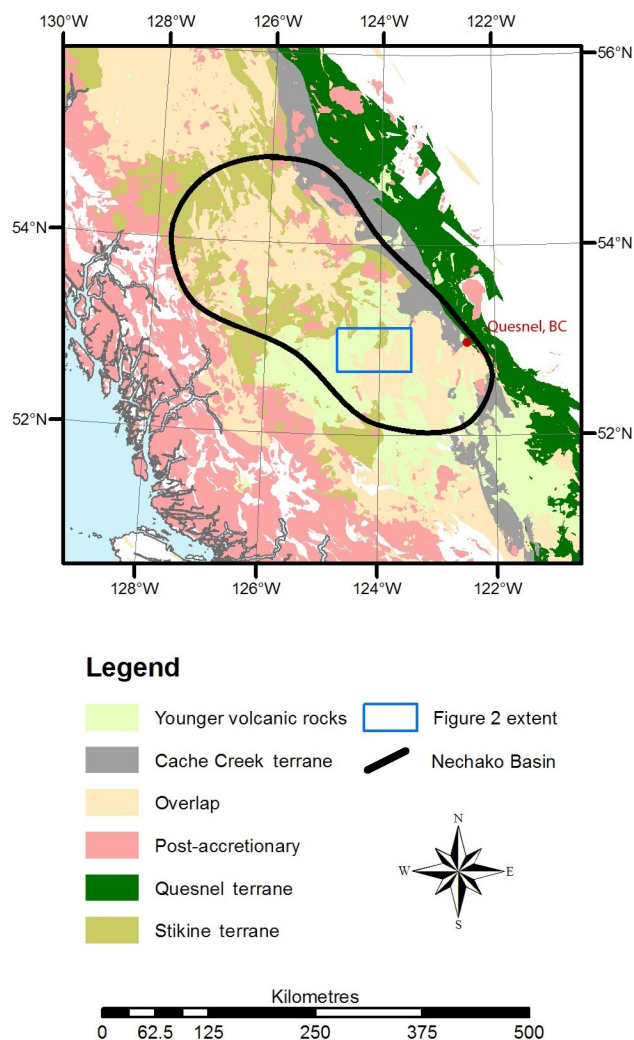


Figure 1. Relevant geological terranes in south-central British Columbia, showing the location of the study area. The Nechako Basin is subdivided into two main regions; this study encompasses the northern edge of the southeastern region, roughly at the boundary between rocks of the Stikine terrane and those of the basin proper (Massey et al., 2005).

hydrocarbon development. Hayes et al. (2003) identified the southeastern portion of the basin as having the highest prospectivity. We carried out waveform-tomography processing of vibroseis data collected along line 10 of the Geoscience BC Nechako Basin seismic survey; please refer to Calvert et al. (2009) for details on data collection. This line is located along the northern boundary of the most prospective region of the Nechako Basin, approximately 100 km west of Quesnel in south-central BC (Figure 2).

The region is underlain by the Stikine terrane, which is composed of marine sediments and volcanic rocks deposited as recently as the Middle Jurassic; the Hazelton Group (Figure 2) is part of the Stikine terrane (Massey et al., 2005). The prospective units for oil and gas exploration in the Nechako Basin are Cretaceous clastic sedimentary rocks, mainly the Skeena Group, that overlie the Stikine

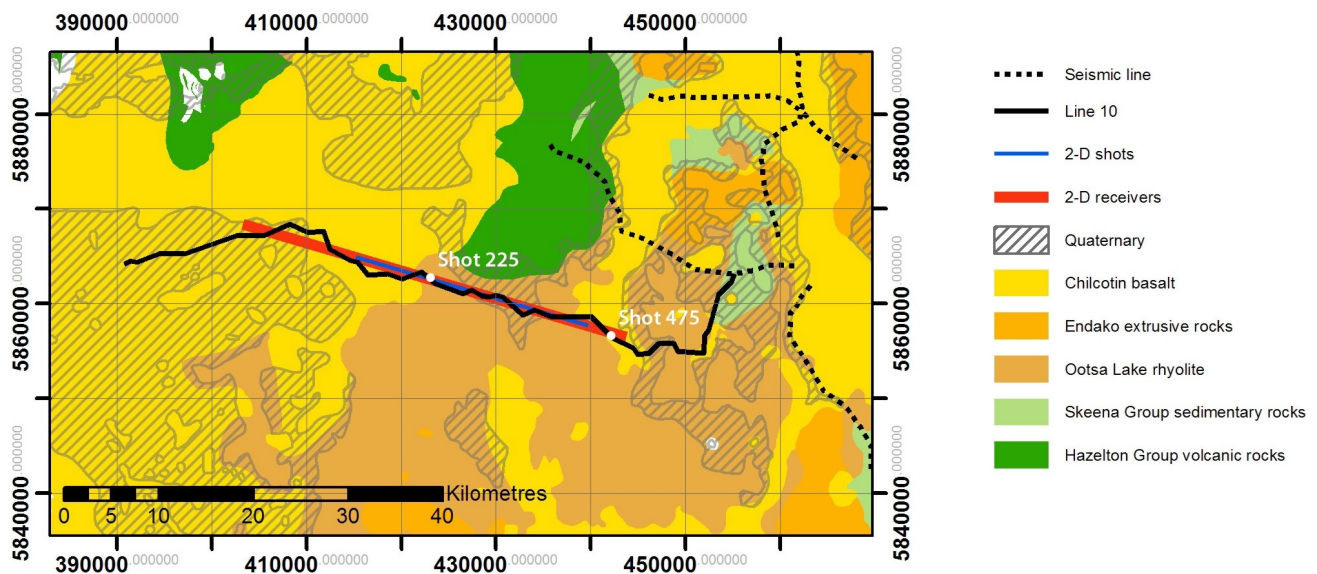


Figure 2. Geometry of seismic line 10 in relation to lithology and several other seismic lines from the 2008 Geoscience BC Nechako Basin vibroseis survey, south-central British Columbia (modified from Smithyman and Clowes, 2010). The surface of the central portion of line 10 is dominated by the Ootsa Lake rhyolite, whereas both flanks are overprinted by the Chilcotin basalt (Massey et al., 2005). To the north, the Hazelton Group volcanic rocks of the Stikine terrane appear to plunge beneath line 10 toward the south. The 2-D approximate geometry used in waveform inversion is highlighted, with corresponding extents of the active source (blue line) and receiver (red line) arrays.

terrane (Hannigan et al., 1994). In turn, these are overlain by non-prospective middle to Late Cretaceous sedimentary rocks as thick as 2500 m within the basin, but these rocks do not outcrop in the region of our study. The near surface is dominated by Eocene volcanic rocks of the Ootsa Lake and Endako groups, followed by the Neogene Chilcotin basalt. Based on rock physics results, the Chilcotin basalt was originally expected to show a higher bulk P-wave velocity than the Ootsa Lake and Endako units. However, recent work by Calvert et al. (in press) indicates that brecciation may cause the Chilcotin basalt to possess slower P-wave velocities throughout much of the region. Quaternary deposits of differing types and varying thicknesses overlie the older rocks (Figure 2).

Geometric Correction and Initial Model

In order to accurately model wave propagation along an irregular land survey geometry, it is necessary to account for 3-D wave propagation, which requires large computational resources. However, with careful pre-processing of the data waveforms, it is possible to account approximately for small off-line geometry errors. In order to model (and invert) the data discussed in this report, we implemented a geometric correction for the data from line 10. This work was carried out since the release of last year's progress report (Smithyman and Clowes, 2010); the differences from the earlier methodology are summarized below.

The first-arrival data were modelled and inverted using First Arrival Seismic Tomography (FAST; Zelt and Barton, 1998) in three dimensions, incorporating the actual geometry

of the survey. However, at each iteration, the velocity model was constrained to be two-dimensional (i.e., the velocity field did not vary perpendicular to the ideal 2-D geometry). We refer to this as a 2.5-D approach. Our motivation was to develop a best-fit 2.5-D velocity model that accounted for the data to an acceptable maximum error and bias (Figure 3a). Once the 2.5-D model was developed, the data were forward modelled using the 3-D and 2-D line geometries. Due to the out-of-plane homogeneity of the velocity model, these results vary only in the sensitivity kernels (i.e., ray paths) of their respective source-receiver pairs. By finding the difference between these two synthetic datasets, we were able to calculate traveltimes shifts for each seismic trace that are necessary to approximate the response from the equivalent 2-D source and receiver geometries (Figure 3b).

It is important to note several limitations to this method:

The traveltimes corrections are derived from the ray equation and therefore are limited by its ability to resolve model parameters. This is valid for common-mode delays, but the sensitivity kernels do not account for events that follow a different path from the first arrivals (e.g., wide-angle reflections).

Small source-receiver offset errors are approximated well, but large traveltimes errors can result from large offsets. This correction is reasonable for traveltimes errors smaller than the RMS misfit of the target data.

Regardless of the efficacy of this correction, the velocities recovered in full-waveform inversion will be somewhat distorted in regions where the line geometry is irregular.

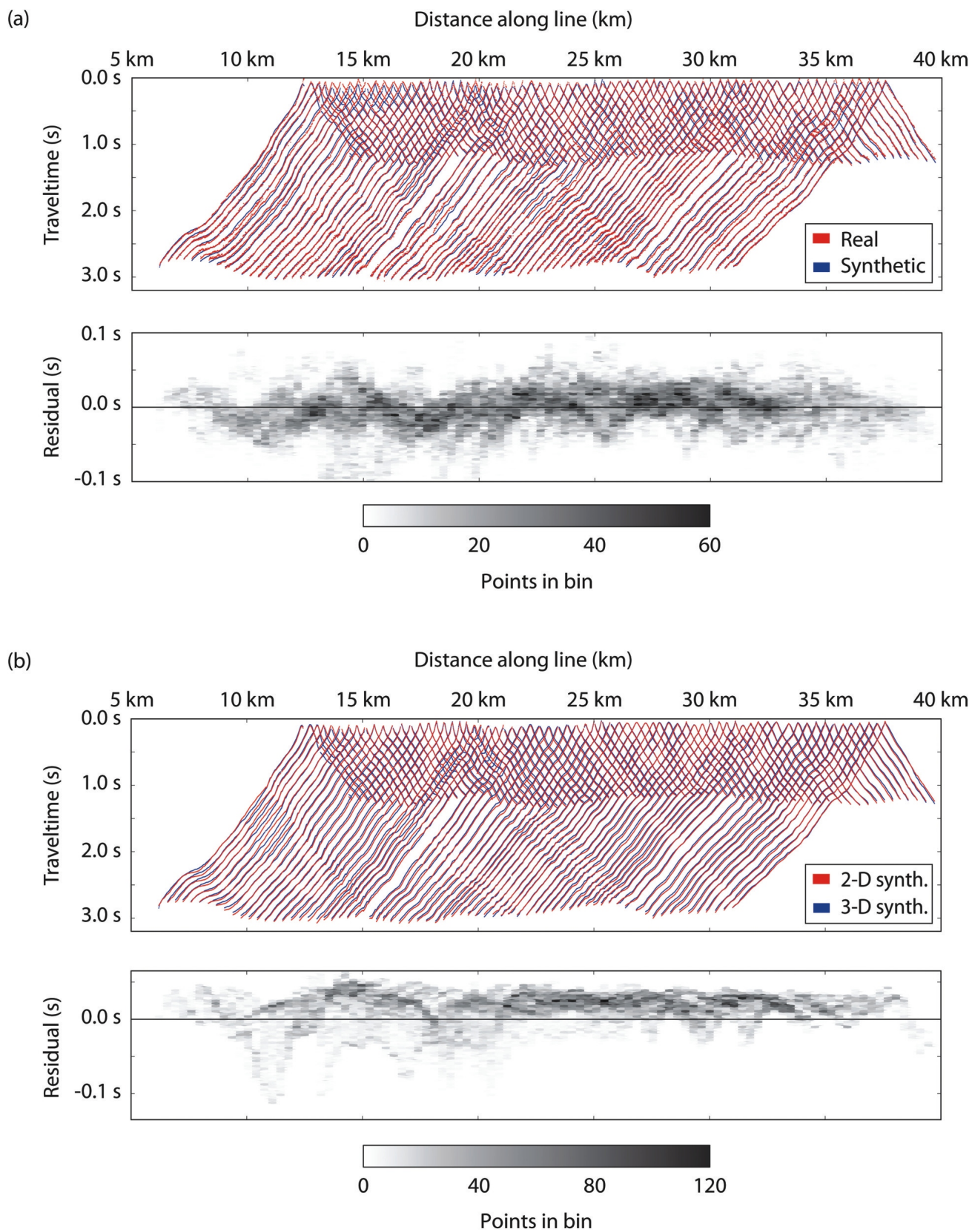


Figure 3. Traveltime and residual plots for seismic line 10 from comparison of **a)** real and 3-D synthetic data, and **b)** 2-D and 3-D synthetic data. The 3-D synthetic data (generated in a 2-D model) predict the true data within an RMS misfit of approximately 27 ms, and the residuals are well distributed about zero mean. The 2-D synthetic data differ from the 3-D synthetic data due to the projection of the geometry onto a plane (striking approximately 106°).

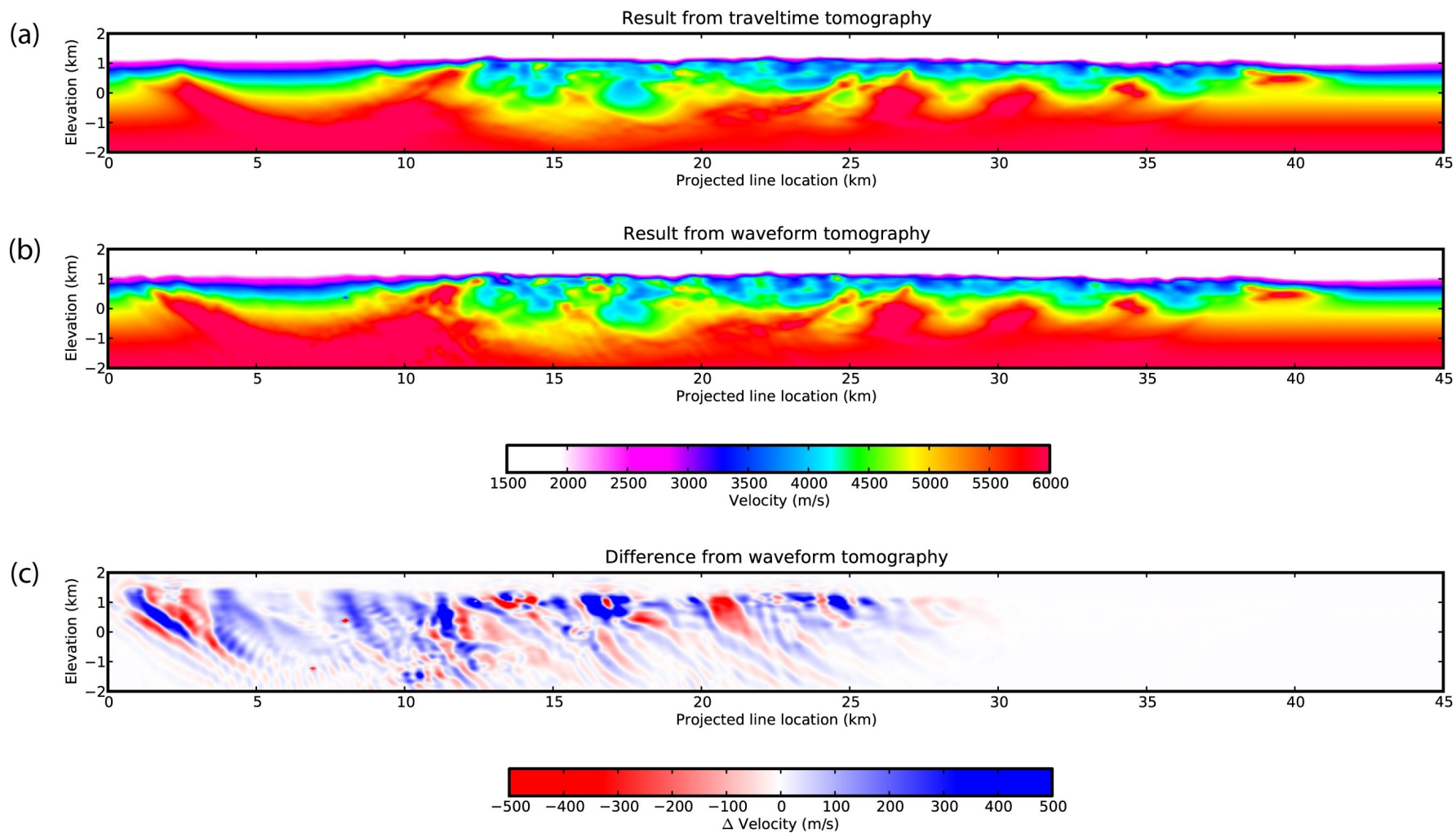


Figure 4. Velocity models for seismic line 10 from traveltimes inversion (a) and subsequent full-waveform inversion (b). The difference (c) is shown to help identify features. The waveform data-fit from traveltimes inversion was excellent in the eastern portion of the model, leading to very small perturbations from full-waveform inversion (see Figure 6).

Results from Waveform Tomography

The velocity model shown in Figure 4a was produced by 2.5-D traveltimes inversion using FAST under the constraints outlined in Smithyman and Clowes (2010) and the previous section. This acted as an input (starting) velocity model for full-waveform inversion. The goal of the full-waveform inversion process was to improve on the velocity model provided by traveltimes inversion in two main ways:

- Spatial resolution can be expected because of the migration-like generation of the model updates.

- Ability to resolve low-velocity zones is possible due to the incorporation of multiple phases and amplitude information.

The aforementioned static corrections were effective at improving the quality of the initial waveform fit. In order to test this, initial synthetic waveforms (also used in inversion) were calculated using a delta function. The initial correspondence between the phase of the real data and synthetic data was high in the eastern portion of line 10 (see Figure 2) but lower towards the west. This is likely due to the large off-line displacements of sources and receivers (relative to the ideal 2-D line) at the western end. Smaller displacements were well accounted for by the time-shifting method.

We carried out full-waveform inversion between 8 and 11 Hz, using an approach in which we iteratively increased the frequency content of the inversion. The initial stages used 8.0, 8.5 and 9.0 Hz frequencies; subsequent stages incorporated data up to 11 Hz. At early stages, a delta function source was used to approximate the response of the ideal broadband vibroseis source. Once frequencies above 9 Hz were incorporated, the inversion proceeded with a synthetic source signature derived directly from the data. The result is presented in Figure 4b, which contrasts with the traveltimes result.

Figure 5 shows a comparison of real and synthetic data from two representative shot gathers in the dataset. This acts as a quality control on the success of the method, and in particular provides valuable information about which features in the model are robust. The data were time windowed for use in the full-waveform inversion processing, and therefore we are particularly interested in data fit within certain specific regions. Analysis of the frequency content of the early arrivals suggests that these data may support additional higher frequencies (up to ~16 Hz) in some parts of the model (e.g., the well-characterized region near shot 475). However, the early-arriving data are very low amplitude above 16 Hz.

Interpretation

The velocity models built by traveltimes tomography and full-waveform inversion can be directly interpreted to as-

ist in developing a geological model of the region. The region of highest confidence in our work is the eastern portion of the line, due to the relatively low line-curvature. Figure 2 presents the surface geological features and Figure 4 shows the velocity model derived for interpretive purposes and any subsequent reflection-data reprocessing (to be done by others). For interpretation, we refer to labels in Figure 6.

The presence of Chilcotin basalt in the eastern portion of the survey region is identified by a local high-velocity anomaly (**A**). This corresponds with rock-physics information suggesting that the Chilcotin basalt is distinguishable by a high seismic velocity relative to the nearby Ootsa Lake and Endako groups. However, recent work (Hayward and Calvert, 2009; Calvert et al., in press) has found that the velocity of the Chilcotin basalt in situ is typically somewhat lower than that of the nearby Eocene volcanics. Note that this is at the far eastern extent of our model, and may not be perfectly resolved. Immediately west of this, there is an apparent increase in the recovered heterogeneity in the near-surface (**B**). This is most likely due to the volcanic rocks underlying the Quaternary cover; however, the variability in velocity likely occurs at a finer scale than we are able to distinguish. This feature appears to correlate well with the distribution of recent surface sediments, extending for about 10 km over the middle eastern portion of the line. Seismic high-velocity features at **C** are interpreted to be due to the Hazelton Group volcanic and volcanoclastic rocks, which outcrop immediately north of line 10. We believe that this unit most likely plunges southward beneath the Eocene volcanic rocks that dominate the near surface. This interpretation corresponds to the knowledge that the basin is deeper towards the south (Hannigan et al., 1994), but it does not preclude the possibility that Hazelton Group outcrops toward the north could be responsible for the high-velocity response. Because of the presence of this feature, we have not attempted to interpret sub-basin structures in this part of the model.

A deepening of the low-velocity region (~3000–3500 m/s) to approximately 700 m (**D**) is interpreted as a sub-basin. This appears, from interpretation of velocities, to be infilled by Ootsa Lake rhyolite, suggesting that the formation of the basin structure is at least Eocene in age. A sharply defined high-velocity feature at **E** could be a volcanic plug. Another sub-basin structure is seen farther west at **F**. However, the confidence of the full-waveform inversion is lower in this region, due to the poorer performance of the 2-D geometry approximation (Figure 2). An 8–10 km wide synformal structure at **G** was initially interpreted to be an artifact of the ray-tracing used in the initial model-building with FAST. More likely, it could be a poorly resolved indication of another sub-basin.

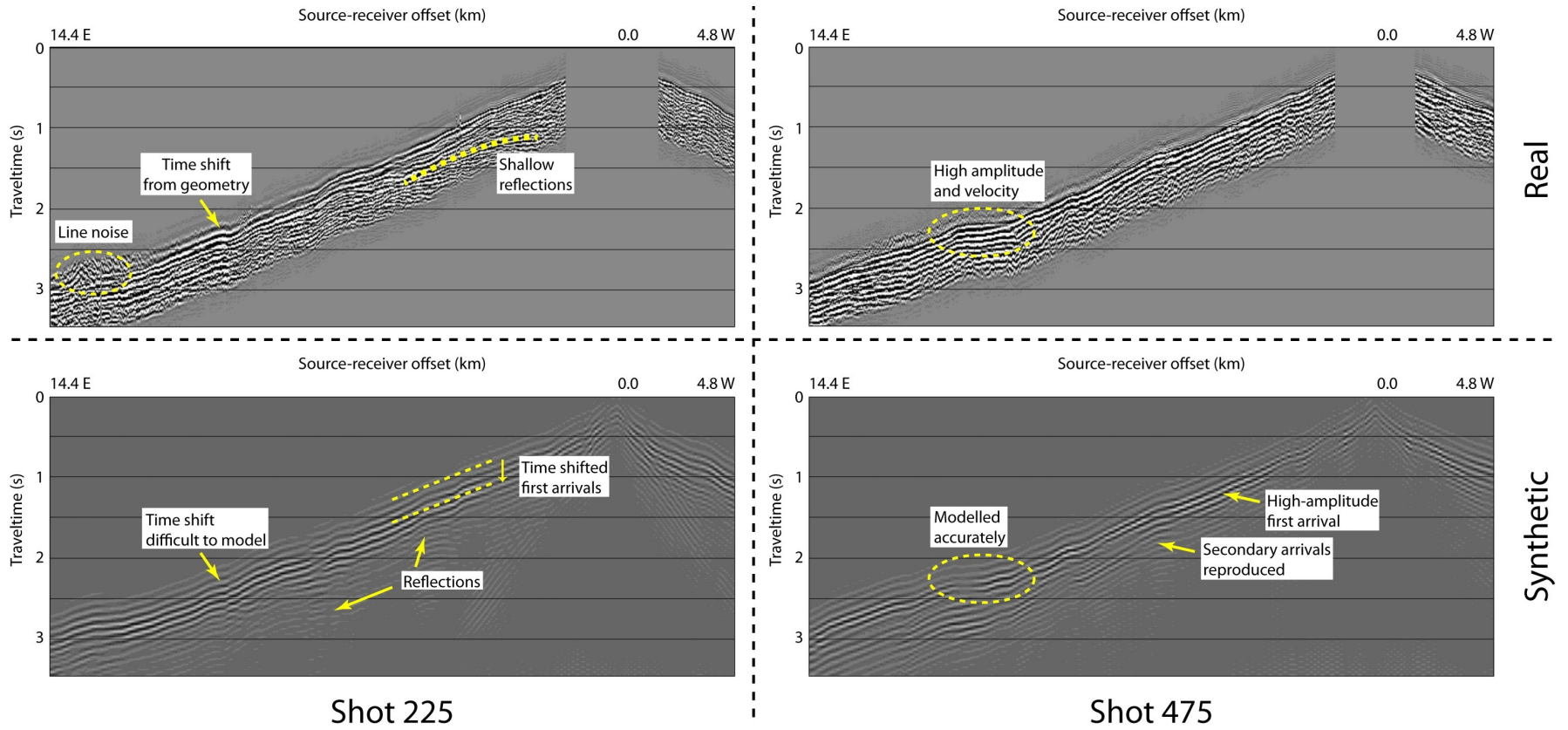


Figure 5. Real (top) and synthetic (bottom) data are shown for two shot gathers on seismic line 10. Shot 225 (left) is representative of the poorer data fit seen in the western portion of the model, due primarily to problems in approximating the geometry. Shot 475 (right) is representative of the high-quality data fit found in the eastern portions of the model. Annotations highlight some of the relevant data features.

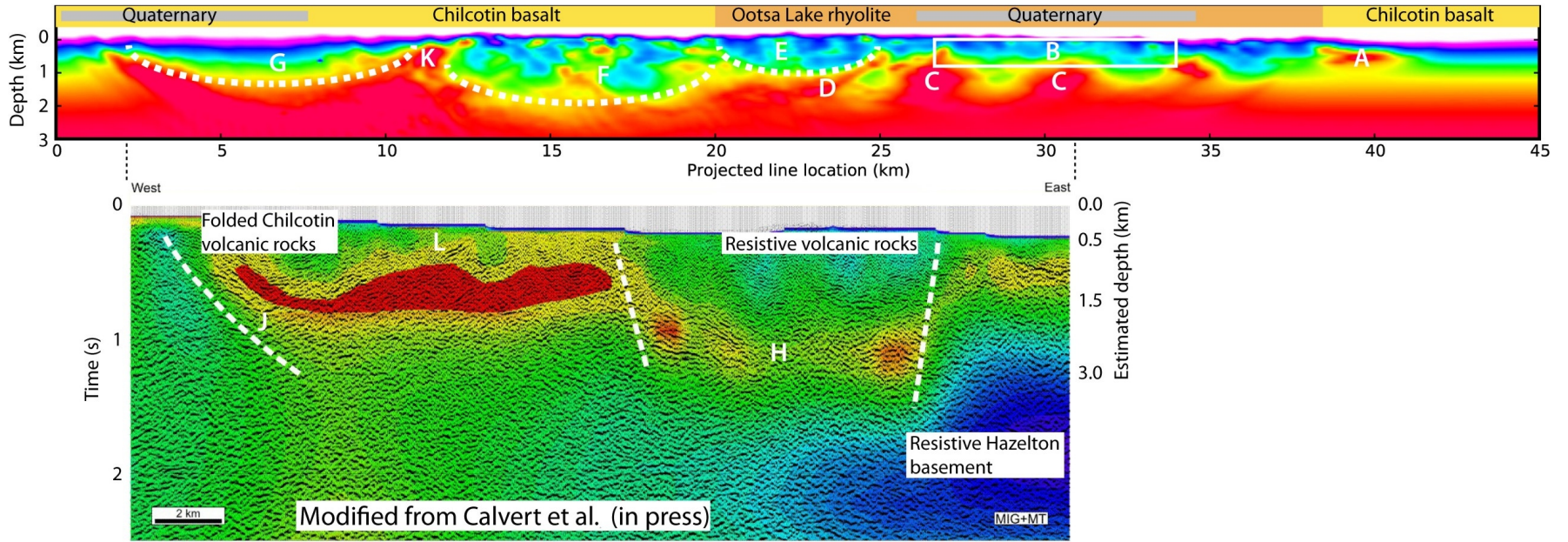


Figure 6. Top: The velocity model for seismic line 10 from Figure 4b is shown annotated with features of interest labelled (described in the text); see Figure 4 for velocity scale bar. **Bottom:** A portion of the migration image is shown with colours overlaid based on magnetotelluric results; labels and an estimated depth scale have been inserted (modified from Calvert et al., in press). Note that the depth scale on the migration image is approximate and likely variable across the image. The horizontal and vertical resolutions are also variable between methods. These models share some complementary features, especially with regard to the identification of sub-basins.

Calvert et al. (in press) present a preliminary interpretation of the vibroseis seismic-reflection sections collected on behalf of Geoscience BC (see Calvert et al., 2009), combined with magnetotelluric information (Spratt and Craven, 2010). The reflection data primarily represent deeper structures than we might expect to see from the first-arrival refraction data alone, but there is a region of overlap where results of the two methods can be directly compared. Additionally, the magnetotelluric results provide information about rock type that is not available from seismic records, although interpretation of results is involved in both cases. Calvert et al. (in press) interpret Eocene and younger extension in the seismic-reflection section through the middle western portion of line 10 (~3–27 km on the scale of Figure 6). They identify highly resistive Hazelton Group basement rocks from magnetotelluric studies in a location that corresponds well with the high-velocity features identified above (**C**). Furthermore, a full-graben structure is interpreted between 16 and 25 km (**H**), and a half-graben east of 3 km (**J**; distances relative to Figure 6). They find evidence for post-Eocene extension in the Chilcotin basalt near surface in the western portion of line 10 (Figure 2), leading to folding and brecciation.

Considering results from Calvert et al. (in press), several additional features of interest may be identified. We see a reasonable correspondence between the graben structure they interpreted at **H** and a deepening of the bedrock interface in our results (**D**, **F**; Figure 6). The geological unit at depth here is not well known, but we presume the presence of Cretaceous sediments between the younger volcanic rocks and Stikinia. The implication is that the graben structure was infilled by Eocene volcanic rocks after or contemporaneous with Eocene extension. However, we identify a high-velocity feature between **D** and **F** that we assume to bound the two sub-basins. Additionally, the sub-basin we identify from velocity information at **D** is significantly shallower than the graben structure identified by Calvert et al. (in press). The feature we interpret at **E** is in a region possessing variable resistivity (Figure 6), but it is not identified in the seismic-reflection interpretation.

Our results show high-velocity near-surface features and heterogeneities (compare the near surface in sub-basins **F** and **D**) that are spatially correlated with the brecciated Chilcotin basalt interpreted by Calvert et al. (in press). However, the full-waveform inversion responsible for producing this heterogeneity in the model was negatively affected by geometry errors in this region, and the exact placement and extent of the heterogeneity are not well constrained. Likewise, we see a high-velocity region at **F** that cannot be well constrained, although the heterogeneity present corresponds to an interpreted fault from the reflection-seismic and magnetotelluric work. The high-velocity feature at **K** seems to have the same orientation and location as a highly

reflective folded package (**L**) in the results of Calvert et al. (in press). Resolution and reliability of our model west of the 10 km point (near **K**, Figure 6) is very degraded, due to the omission of back-shots beyond this point; however, we have included it for comparison with Calvert et al. (in press) and future works.

Conclusions and Future Work

From waveform tomography of the first arrivals and waveform data, we produced a detailed near-surface velocity model along line 10 of the Geoscience BC Nechako Basin seismic survey. This compares favourably with other methods in terms of the ability to resolve near-surface features. In particular, the use of a wide range of source-receiver offsets and dense spatial sampling allows more advanced processing than conventional refraction statics. We interpreted these results and compared them with interpretations by other researchers based on near-offset seismic-reflection and magnetotelluric methods. The combined interpretation of these data and other multidisciplinary research presents the best chance to model the geology of the complex Nechako Basin. Based on work to date, there is evidence for the presence of shallow sub-basins in the region of interest.

We expect to continue applying waveform tomography to other datasets in the Nechako Basin and contribute results to the ongoing interpretation of the geology. This will likely include production of a detailed fence-diagram model that ties together information from multiple seismic lines. To further constrain the results of this method, we intend to compare our results with detailed structural geology information where available.

Acknowledgments

We appreciate the support received from Geoscience BC in carrying out this research. Thanks also go to the Natural Sciences and Engineering Research Council of Canada (NSERC) for funding this and ongoing research through the Canadian Graduate Scholarships program. We deeply appreciate discussions and technical support from A. Calvert and his associates at Simon Fraser University, and G. Pratt's group at the University of Western Ontario. Feedback from P. Hammer (University of British Columbia) and A. Calvert was extremely helpful in preparing this manuscript.

References

- Calvert, A.J., Hayward, N., Smithyman, B.R. and Takam Takougang, E.M. (2009): Vibroseis survey acquisition in the central Nechako Basin, south-central British Columbia (parts of NTS 093B, C, F, G); *in* Geoscience BC Summary of Activities 2008, Geoscience BC, Report 2009-1, p. 145–150, URL <<http://www.geosciencebc.com/s/SummaryofActivities.asp?ReportID=358404>> [November 2010].

- Calvert, A.J., Hayward, N., Spratt, J.E. and Craven, J.A. (in press): Seismic reflection constraints on upper crustal structures in the volcanic-covered central Nechako Basin, British Columbia; *Canadian Journal of Earth Sciences*.
- Hannigan, P., Lee, P., Osadetz, K., Dietrich, J. and Olsen-Heise, K. (1994): Oil and gas resource potential of the Nechako-Chilcotin area of British Columbia; BC Ministry of Forests, Mines and Lands, GeoFile 2001-6, 167 p.
- Hayes, B.J., Fattahi, S. and Hayes, M. (2003): The Nechako Basin—frontier potential close to home (abstract); unpublished paper presented at Canadian Society of Petroleum Geologists, 2003 Annual Convention, URL <www.cspg.org/conventions/abstracts/2002abstracts/051S0118.pdf> [November 2009].
- Hayward, N. and Calvert, A.J. (2009): Eocene and Neogene volcanic rocks in the southeastern Nechako Basin, British Columbia: interpretation of the Canadian Hunter seismic reflection surveys using first-arrival tomography; *Canadian Journal of Earth Sciences*, v. 46, no. 10, p. 707–720.
- Massey, N.W.D., MacIntyre, D.G., Desjardins, P.J. and Cooney, R.T. (2005): Digital map of British Columbia: whole province; BC Ministry of Forests, Mines and Lands, GeoFile 2005-1.
- Pratt, R.G. (1999): Seismic waveform inversion in the frequency domain, part 1: theory and verification in a physical scale model; *Geophysics*, v. 64, p. 888–901.
- Pratt, R.G. and Gouly, N.R. (1991): Combining wave equation imaging with traveltome tomography to form high resolution images from cross-hole data; *Geophysics*, v. 56, p. 208–224.
- Pratt, R.G. and Worthington, M.H. (1990): Inverse theory applied to multi-source cross-hole tomography, part 1: acoustic wave-equation method; *Geophysical Prospecting*, v. 38, p. 287–310.
- Smithyman, B.R. and Clowes, R.M. (2010): Improved near-surface velocity models from the Nechako Basin seismic survey, south-central British Columbia (parts of NTS 093B, C, F, G), part 1: traveltome inversions; *in* Geoscience BC Summary of Activities 2009, Geoscience BC, Report 2010-1, p. 227–234, URL <<http://www.geosciencebc.com/s/SummaryofActivities.asp?ReportID=379075>> [November 2010].
- Spratt, J. and Craven, J. (2010): Magnetotelluric imaging of the Nechako Basin, British Columbia; *in* Current Research 2010-3, Geological Survey of Canada, 9 p., URL <http://geopub.nrcan.gc.ca/moreinfo_e.php?id=261488> [November 2010].
- Zelt, C.A. and Barton, P.J. (1998): 3D seismic refraction tomography: a comparison of two methods applied to data from the Faeroe Basin; *Journal of Geophysical Research*, v. 103, p. 7187–7210.